9. D. W. R. McKinley, *Meteor Science and Engineering* (McGraw-Hill, New York, 1961).
10. D. M. Hunten, R. P. Turco, O. B. Toon, *J. Atmos. Sci.* **37**, 1342 (1980).
11. G. C. Hess and M. A. Geller, *Aeron. Rep. 74* (Aeronomy Laboratory, Department of Electrical and Computer Engineering, University of Illinois, Urbana, 1976).
12. D. W. Hughes, *Space Res.* **15**, 531 (1975).
13. V. A. Bronshten, *Physics of Meteoric Phenomena* (Reidel, Dordrecht, Holland, 1983).
14. J. M. C. Plane, *Int. Rev. Phys. Chem.* **10**, 55 (1991).
15. T. J. Kane and C. S. Gardner, in preparation.
16. D. W. Hughes, in *Cosmic Dust*, J. A. M. McDonnell, Ed. (Wiley, New York, 1978), pp. 148–157.
17. J. T. Wasson and F. T. Kyte, *Geophys. Res. Lett.* **14**, 779 (1987).

18. We thank T. J. Beatty, R. E. Bills, R. L. Collins, C. A. Hostetler, W. M. Pfenninger, J. Qian, D. C. Senft, and D. R. Scherrer for help in system development and data acquisition. This work was supported in part by NSF grants ATM 88-11771, ATM 90-24367, and ATM 90-01511.

1 September 1992; accepted 23 December 1992

Isomers of Small Carbon Cluster Anions: Linear Chains with up to 20 Atoms

Gert von Helden, Paul R. Kemper, Nigel G. Gotts,
Michael T. Bowers*

The structure of small carbon cluster anions, C_n^- ($4 \leq n \leq 20$), was investigated with the use of ion chromatography. With this technique, both the existence and the relative amounts of possible structural isomers can be determined. More than 99% of the ions C_5^- to C_9^- were found to be linear under these experimental conditions. Starting with C_{10}^-, a monocyclic isomer was observed, and linear and moncyclic structures coexisted from C_{10}^- through at least C_{20}^-. This result is in contrast to previous work on positive ions, which showed the existence of linear isomers from C_5^+ to C_{10}^+, with linear and cyclic isomers coexisting only from C_7^+ to C_{10}^+. Above C_{10}^+, no linear clusters were observed.

During the last several years, considerable research effort has been directed toward understanding the structures and properties of small clusters. Small carbon clusters are especially interesting because of their possible importance in combustion and pyrolysis processes (*1*), their importance in astrophysical processes (*2*), and their role in the formation and growth of fullerenes. Because of their high reactivity, most carbon clusters cannot be isolated in macroscopic quantities and analyzed by traditional means. As a consequence, little is known about the structure of most clusters. Some structural information has been deduced from size distributions in mass spectra (*3*) and metastable reactions in mass spectrometers (*4*), reactivity studies (*5*), computational studies (*6–8*), and various spectroscopic techniques (*9*). Photoelectron spectroscopy (*10, 11*) shows the presence of linear clusters for cluster anions with as many as nine atoms and suggests that larger clusters have monocyclic ring structures with the possibility of both linear and cyclic structures being present in C_{10}^- and C_{11}^-. Even with these results, it has remained unclear if cyclic cluster anions exist with less than 10 atoms or if linear clusters exist with more than 11 atoms and if there is a region where linear and cyclic clusters coexist. Coulomb explosion experiments (*12*) have shown the possible presence of different isomers for C_4^-, C_5^-, and C_6^-. A review on the research up to 1989 has been given by Weltner and van Zee (*9*).

We recently introduced the technique of ion chromatography and applied it to carbon cluster cations (*13*). This technique, in combination with computer modeling, allows us to probe the shape and possible existence of structural isomers for small cluster ions. Various families of structural isomers have been identified for carbon cluster cations (*13–15*). Here, we present results from similar studies on carbon cluster anions that contained from 4 to 20 atoms.

The experimental setup has been described previously (*16*), and only a brief outline is given here. A schematic of the apparatus is shown in Fig. 1. Carbon cluster anions are generated in a standard laser vaporization–supersonic expansion cluster source. A pulse of photons from an excimer laser impinges on a continuously rotating and translating graphite rod. The pulse is timed to coincide with a burst of helium, which is admitted from a pulsed valve. Carbon clusters exit the source through a 30-degree conical nozzle after traveling through a channel that is 3 mm in length and 2 mm in diameter. In some experiments, a spacer is inserted to increase the channel length to 8 mm. No further ionization is used. Cluster anions are accelerated to 5 keV and then mass-selected by a reverse geometry, double-focusing mass spectrometer. An electric shutter cuts a short pulse (2 to 10 μs) of ions out of the ≈40-μs mass-selected ion packet and injects it at low energies (2 to 15 eV) into a high-pressure drift cell (Fig. 2) filled with helium at 2 to 5 torr. A small electric field (2 to 20 V/cm) pulls the ions gently through the cell. Ions exiting the cell are passed through a quadrupole mass filter and are detected as a function of time. The resulting arrival time distribution (ATD) is collected on a multichannel scaler. The time an ion spends in the cell is inversely proportional to the mobility of the ion and directly proportional to the average cross section of the ion. Ions of the same mass but with different structures may have different mobilities. Structures with a large average cross section have a lower mobility

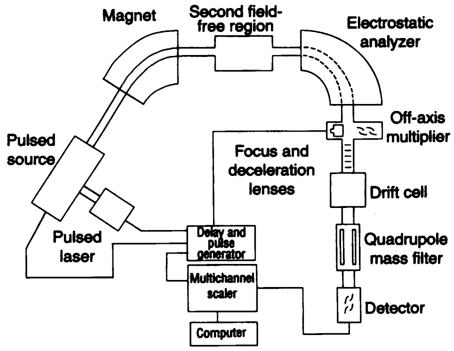

Fig. 1. Schematic of the overall ion chromatography instrument. Carbon cluster ions are generated by laser vaporization–supersonic expansion. Ions are mass-selected by the magnet and electrostatic analyzer and injected at low energy into the chromatography cell. Ions exiting the cell pass a quadrupole mass filter and are detected by standard ion counting techniques.

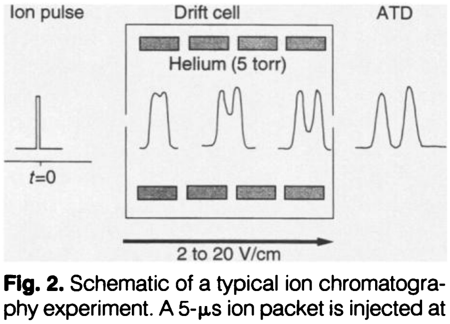

Fig. 2. Schematic of a typical ion chromatography experiment. A 5-μs ion packet is injected at low energy into the high-pressure drift cell. Ions drift through the cell under the influence of a weak electric field. Different structural isomers are separated because of their different collision cross section (size). Ions exiting the cell are recorded, and their ATDs are obtained. Typical drift times (*t*) in our cell were 100 to 1000 μs.

Department of Chemistry, University of California, Santa Barbara, CA 93106.

*To whom correspondence should be addressed.

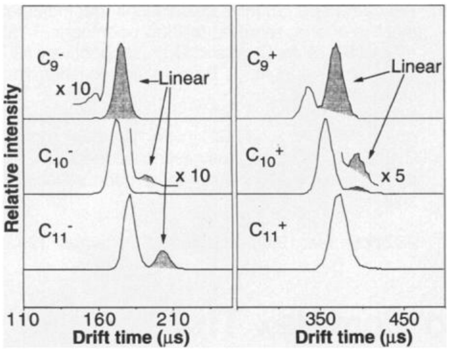

Fig. 3. Typical ATDs for carbon cluster ions with 9, 10, and 11 atoms. Shown on the left are results from carbon cluster anions and on the right previous results for carbon cluster cations (*15*). Drift times for positive and negative ions differ because of different experimental conditions. Peaks that resulted from linear isomers are shown shaded; unshaded peaks resulted from cyclic isomers.

and exit the cell at later times than compact structures with small cross sections. These different structures therefore can show up as different peaks in the ATD. Both the relative amount of the separated structures and their mobilities can be determined.

The ATDs for 9–, 10–, and 11–carbon atom clusters are shown in Fig. 3. These ATDs are bimodal for all cases except C_{11}^+. Each ATD can be fit with a theoretical model in order to obtain the ionic mobility and the relative isomer abundance. The inverse mobility of the different carbon cluster ions containing from 4 to 20 atoms is shown in Fig. 4. For the cations, extensive computer simulations of mobilities and experiments with linear and cyclic hydrocarbon cations has shown (*13–15*) that the isomers in this size range correspond to linear and cyclic clusters with cyclic clusters appearing at shorter times in the ATD. Because the mobilities of the corresponding anion isomers were almost exactly the same as those of the cations of the same size, it is safe to say that the two peaks in the ATDs were attributable to the presence of linear and cyclic structures.

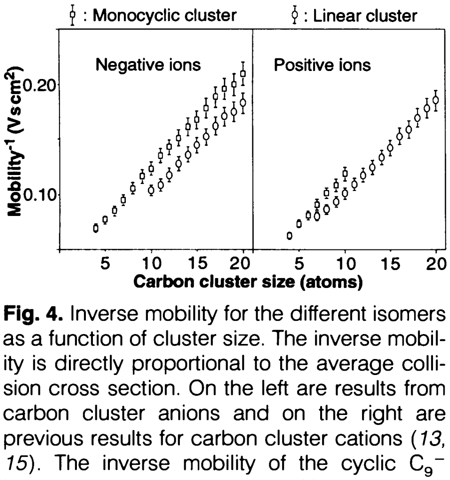

Fig. 4. Inverse mobility for the different isomers as a function of cluster size. The inverse mobility is directly proportional to the average collision cross section. On the left are results from carbon cluster anions and on the right are previous results for carbon cluster cations (*13, 15*). The inverse mobility of the cyclic C_9^- isomer is not shown because of its low relative abundance. Note that for the anions, linear isomers are present from C_5^- to C_{20}^-.

Cyclic carbon cluster anions were present in our experiment from C_9^- to C_{20}^- and beyond, with the amount of cyclic isomer in C_9^- always less than 1%. Linear isomers exist from C_5^- to more than C_{20}^-. Theoretical mobility studies on linear and cyclic carbon cluster cations indicated that cyclic and linear isomers could be resolved for C_5^- and larger clusters but most likely not for C_4^-. The C_4^- molecule could therefore exist in our experiment as linear, cyclic, or both. Starting at C_{20}^-, a new isomer appeared at shorter times than the moncyclic ring; this isomer is the start of a new series of bicyclic structures (*17*). For isomers to C_{11}^-, the observed isomer abundances were in qualitative agreement with the photoelectron studies of Yang *et al.* (*10*) and Arnold *et al.* (*11*). In both studies, the photoelectron spectra could be interpreted as being composed of linear clusters up to C_9^-, with C_{10}^- being cyclic and C_{11}^- having linear and cyclic isomers. C_5^-, C_6^-, and C_8^- may also contain some cyclic isomer (*11*); Arnold *et al.* used an ion source of a design similar to that used in our work. Under our experimental conditions, less than 0.1% of these clusters were cyclic.

One of our most interesting results is that linear carbon cluster anions were observed as large as C_{20}^-. In contrast to these findings, no linear positive ion cluster has been observed greater than C_{10}^+. Also, the first cyclic isomer appeared at C_7^+, with linear and cyclic clusters coexisting only up to C_{10}^+, whereas the first cyclic anion appeared at C_{10}^-. These results indicate that the charge state of the cluster has an important function in structure stability, at least for small clusters. These differences between positive and negative ions can in part be explained by the different electron affinities and ionization potentials of linear and cyclic clusters. For example, cyclic C_{10} has a electron affinity of 2.2 ± 0.1 eV (*11*), whereas linear C_{10} has an electron affinity of about 4.6 eV (*8*). This difference yields a greater stabilization of 2.4 eV for the linear cluster upon electron attachment. For the positive ions, the stabilization (that is, the difference in ionization potentials) of the linear and the cyclic clusters of C_{10}^+ is only ~0.8 eV (*18*). This situation is probably similar for other linear and cyclic clusters, so that it comes as no surprise that linear clusters larger than those found in the cations were observed in the anions.

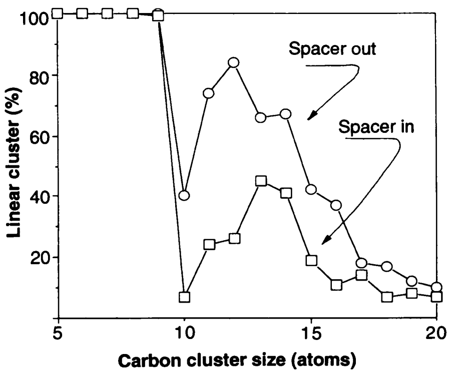

Fig. 5. Abundance of linear carbon cluster isomers as a function of cluster size for two different ion source configurations. Data points in squares were taken with an ion source that includes a 5-mm spacer between the source body and the nozzle; data points in circles resulted from an ion source without the spacer. The spacer extended the residence time of the ions in the ion source.

The percentage of linear isomer as a function of cluster size for two different ion source configurations is shown in Fig. 5: one set of experiments includes the 5-mm spacer and the second has no spacer between the source body and the nozzle. In both curves, the linear isomers have a strong minimum at C_{10}^-. The percentage of linear clusters proceeds to a maximum at around C_{12}^- and subsequently falls off almost monotonically. Insertion of the 5-mm spacer reduced the fractional abundance of linear isomer, whereas the qualitative shape of the curves was relatively unaffected.

To understand the relative abundances of cyclic and linear clusters, one must consider two factors: the kinetic processes for formation and the depletion of clusters in the ion source and the relative stabilities of the isomers. The 5-mm spacer would affect the residence time of the ions in the source and therefore influence the kinetics in the source and possibly the internal energy of the clusters. The formation rates are expected to be a strong function of variables such as helium pressure and the residence time in the source. The linear clusters are expected to react quickly with neutral carbon clusters because of the presence of two reactive sites. Reactions of small neutral units with these sites might proceed with almost no barrier because no bonds would be broken in the course of reaction. Cyclic clusters, on the other hand, would be much less reactive (*19*) because all atoms are only bonded to their two nearest neighbors. The reaction of cyclic clusters with other clusters is thus likely to involve barriers on the reaction surface. The expected result, as seen in the data in Fig. 5, is a depletion of linear clusters with longer source residence times.

The stability of the cluster is also expected to have a strong effect on the observed isomer distribution. For clusters with more than a few atoms, the potential energy surface is very complex, with many local minima often separated by large barriers. One consequence is that clusters need long annealing times to attain thermodynamic equilibrium. The transformation of cyclic clusters to linear clusters, for example, requires breaking a C–C bond, which implies a large barrier, especially for large cyclic clusters with little bond strain (*20*). We therefore did not expect the different isomers to be in thermodynamic equilibrium when leaving the source. Nonetheless, longer residence times in the ion source, under relatively high temperature conditions, would increase the annealing time and might shift the isomer distribution toward the thermodynamically more stable isomers.

Finally, the fact that C_n^- clusters exist in relatively large sizes suggests that neutral linear carbon clusters might also exist in this size range, because the most plausible mechanism for anion formation is electron attachment to neutral clusters. Our data do not directly address this issue, but the surprisingly large abundance of linear C_n^- species for $11 \leq n \leq 16$ supports this interpretation.

REFERENCES AND NOTES

1. P. Gerhardt, S. Loffler, K. H. Homann, *Chem. Phys. Lett.* **137**, 306 (1987).
2. P. F. Bernath, K. H. Hinkle, J. J. Keady, *Science* **244**, 562 (1989).
3. M. D. Cox, K. C. Reichmann, A. J. Kaldor, *J. Chem. Phys.* **88**, 1588 (1988).
4. P. P. Radi, T. Bunn, P. R. Kemper, M. Molchan, M. T. Bowers, *ibid.*, p. 2809.
5. S. W. McElvany, W. R. Creasy, A. O'Keefe, *ibid.* **85**, 632 (1986); S. W. McElvany, B. I. Dunlap, A. O'Keefe, *ibid.* **86**, 715 (1987); S. W. McElvany, *ibid.* **89**, 2063 (1988); *Int. J. Mass Spectrom. Ion Processes* **102**, 81 (1990); P. A. Hintz, M. B. Sowa, S. L. Anderson, *Chem. Phys. Lett.* **177**, 146 (1991).
6. K. Raghavachari and J. S. Binkley, *J. Chem. Phys.* **87**, 2191 (1987); V. Parasuk and J. Almlöf, *Chem. Phys. Lett.* **184**, 187 (1991).
7. C. Liang and H. F. Schaefer III, *J. Chem. Phys.* **93**, 8844 (1990); M. Feyereisen, M. Gutowski, J. Simons, J. Almlöf, *ibid.* **96**, 2926 (1992).
8. J. D. Watts and R. D. Barlett, *ibid.* **97**, 3445 (1992).
9. W. Weltner and R. van Zee, *Chem. Rev.* **89**, 1713 (1989).
10. S. H. Yang, C. L. Pettiette, J. Conceicao, O. Cheshnovsky, R. E. Smalley, *Chem. Phys. Lett.* **144**, 431 (1988).
11. D. W. Arnold, S. E. Bradforth, T. N. Kitsopoulos, D. E. Neumark, *J. Chem. Phys.* **95**, 8753 (1991).
12. Z. Vager *et al.*, *Z. Phys. D* **19**, 413 (1991); D. Zajfman *et al.*, *Science* **258**, 1129 (1992).
13. G. von Helden, M. T. Hsu, P. R. Kemper, M. T. Bowers, *J. Chem. Phys.* **95**, 3835 (1991).
14. _____, in *Proceedings of the SPIE Conference on Applied Spectroscopy in Materials Science II*, Los Angeles, CA, January 1992, W. G. Golden, Ed. (SPIE, Bellingham, WA, 1992), vol. 1636, pp. 182–189.
15. _____, in *Proceedings of the Symposium on Novel Forms of Carbon*, Material Research Society Conference in San Francisco, CA, May 1992, D. Cox, Ed. (Material Research Society, Pittsburgh, PA, in press).
16. P. P. Radi, G. von Helden, M. T. Hsu, P. R. Kemper, M. T. Bowers, *Int. J. Mass Spectrom. Ion Processes* **109**, 49 (1991).
17. G. von Helden, P. R. Kemper, N. G. Gotts, M. T. Bowers, unpublished results.
18. Estimated from the HOMO (highest occupied molecular orbital) orbital energies given in (*7*) by Koopmans theorem.
19. We measured reaction rate constants for both linear and cyclic C_7^+ to C_{10}^+ with a series of small molecules, and in all cases the cyclic isomer was much less reactive (*5*).
20. We carried out ab initio calculations that indicate that the energy required for ring opening is 3.75 eV and 3.5 eV for C_{10}^+ and C_{11}^+, respectively (G. von Helden and M. T. Bowers, unpublished results).
21. Support by Air Force Office of Scientific Research grant AFOSR 92-J-0021 and by NSF grant CHE91-19752 is gratefully acknowledged. G.v.H. thanks the IBM Corporation for a graduate fellowship.

28 September 1992; accepted 22 December 1992

A Mixed-Valent Polyiron Oxo Complex That Models the Biomineralization of the Ferritin Core

Kingsley L. Taft, Georgia C. Papaefthymiou, Stephen J. Lippard*

A novel polyiron oxo complex, $[Fe^{III}_4Fe^{II}_8(O)_2(OCH_3)_{18}(O_2CCH_3)_6(CH_3OH)_{4.67}]$ (1), has been prepared from ferrous acetate and lithium methoxide in methanol by slow addition of dioxygen. The three-dimensional close-packed layered structure found in 1 closely mimics that proposed for the inorganic core in the iron storage protein ferritin. The Mössbauer spectra of 1 reveal superparamagnetic relaxation at temperatures below 15 K, a property characteristic of the ferritin core. The small size and mixed-valent nature of 1 suggest that it is a reasonable model for intermediates formed in the biomineralization of iron during ferritin core formation. A related compound, with the same iron-oxygen framework found in 1 but containing only two ferric ions, has also been structurally characterized. Because the clusters exhibit properties of both discrete molecules and extended solids, they are representative of a new class of nanometer-sized compounds that bridge the molecular solid-state boundary.

Iron homeostasis is maintained in part by the iron storage protein ferritin (Ft), which is comprised of a highly symmetrical coat consisting of 24 polypeptide subunits that can encapsulate up to 4500 iron atoms in an iron oxide hydroxide core (*1–3*). This iron(III) mineral core is formed inside the preassembled protein shell upon oxidation and hydrolysis of iron(II). The structure of the iron core of Ft and the related mineral ferrihydrite is believed to consist of close-packed layers of oxygen atoms with iron occupying octahedral interstitial sites (*4–6*). Here we report the preparation and characterization of $[Fe^{III}_4Fe^{II}_8(O)_2(OCH_3)_{18}(O_2CCH_3)_6(CH_3OH)_{4.67}]$ (**1**), the structural, Mössbauer, and magnetic properties of which resemble ferrihydrite and the Ft core. Features of **1** are also realized in several other inorganic compounds, including the polyoxometalates (*7*), mixed-valent iron-containing minerals (*8*), and a variety of partially oxidized iron oxide hydroxides known as "green rusts" (*5, 6*). The characterization of **1** may help to clarify the nature of the iron core in Ft; its synthesis may serve to mimic features of the biomineralization process by which this core is deposited (*9*).

Ferrous ion dissolved in strongly basic methanol solutions reacts rapidly with excess dioxygen to give intractable yellow precipitates. In contrast, slow diffusion of dioxygen into methanol solutions of ferrous acetate and lithium methoxide yields dark blue-green rectangular crystals of **1** (*10*). The molecular structure of **1**, as determined by x-ray crystallography at 186 K, is comprised of 12 edge-shared FeO_6 octahedra (Fig. 1) (*11*). From charge and bond-distance criteria, atoms Fe(1), Fe(1)′, Fe(2), and Fe(2)′ are assigned as ferric ions. All of the iron atoms except for the two outermost ones, Fe(6) and Fe(6)′, are coordinated to the two central oxide anions. The remaining coordination sites are filled by methoxide, acetate, and methanol ligands.

Compound **1** has a distorted sodium chloride structure type, with the oxygen atoms arranged in a cubic close-packed array and the iron atoms residing in octahedral interstices (Fig. 2). Thus, the polyiron oxo molecule has a three-dimensional lattice structure of iron and oxygen atoms like that proposed for Ft and ferrihydrite. Other characterized polyiron complexes have either a layer or cluster motif, because they do not contain the μ_6-oxo ligands needed to form the lattice array of compound **1** (*12–15*). One exception is the structure that occurs in two related hexanuclear iron(III) complexes, each of which

---

K. L. Taft and S. J. Lippard, Department of Chemistry, Massachusetts Institute of Technology, Cambridge, MA 02139.
G. C. Papaefthymiou, Francis Bitter National Magnet Laboratory, Massachusetts Institute of Technology, Cambridge, MA 02139.

*To whom correspondence should be addressed.